Permeability measurements and precipitation sealing of basalt in an ancient exhumed subduction-zone fault

Aitaro Kato[1), 2)]*, Arito Sakaguchi[1)], Shingo Yoshida[2)], Hiromine Mochizuki[2)] and Yoshiyuki Kaneda[1)]

[1)] The Institute for Frontier Research on Earth Evolution, Japan Marine Science and Technology Center, Yokosuka, Japan
[2)] Earthquake Prediction Research Center, Earthquake Research Institute, The University of Tokyo, Tokyo, Japan

Abstract

We conducted permeability measurements of basalt sampled from an exhumed ancient fault zone in the Cretaceous Shimanto accretionary complex in Japan, in order to investigate permeability structure and evolution following shear failure. Permeability showed a strong reduction with increase in the effective confining pressure and temperature. Rapid sealing at elevated temperatures was observed during hold experiments following shear failure. The results indicate that the permeability of a subduction megathrust fault would rapidly decrease due to the precipitation of clay-like minerals and other minerals, and indicates the potential for high fluid pressure in fault zones.

Key words : permeability, sealing, basalt, seismogenic environment, ancient fault zone

Introduction

Our understanding of the mechanics of subduction thrust faults is limited by a lack of information on the mechanical properties of fault zones. A major goal of the IODP drilling program is direct sampling by drilling into the seismogenic zone of an active plate boundary fault system. The drilling plan is framed around a set of specific hypotheses, derived from key questions in fault mechanics and earthquake physics. These key questions are cited as follows. "What processes and mechanisms control the transitions from stable to unstable slip that define the seismogenic zone in subduction megathrusts?". "What is the nature of the asperity ?". "What causes the apparent weakness of subduction thrusts ?". "What are the physical properties of fault zone materials and the surrounding damage zone?" [*Nankai Trough Seismogenic Zone Research Group*, 2001]. In order to answer these questions, we need to conduct the following laboratory studies under *in situ* conditions using core samples collected from a

fault zone and its surroundings : (1) shear strength of the fault zone and surrounding rocks, (2) instability or stability of fault slip, (3) permeability structure for understanding pore fluid pressure in seismogenic zones, (4) seismic velocity structure, and (5) electronic conductivity structure. An investigation of these properties of fault rocks will certainly lead to a deeper understanding of fault mechanics. Furthermore, outcomes from laboratory experiments using IODP core samples will provide valuable information for simulating the earthquake generation process.

Until now, it has been possible to evaluate shear strength, stability-instability of fault slip, and permeability in seismogenic environments (pore water pressure, temperature) for a shear failure of intact rock and frictional sliding on pre-cut faults [*e.g.,* Blanpied *et al.,* 1998 ; Kato *et al,* 2003]. These experiments, however, used quarried rocks, such as granites and sand stones, not fault rock under *in situ* conditions. It is extremely difficult to evaluate physical properties such as shear strength and stability-

instability of slip of fault rock *in situ.* We, therefore, need fault materials from an active fault system to determine the physical properties of a subduction-zone fault.

Morrow and Lockner [2001] conducted shear failure and sliding experiments using representative rocks available from outcrops from a number of formations adjacent to the Hayward fault zone. They found that the peak shear strength of the rocks increases with effective confining pressure, and the frictional coefficient (0.6〜0.85) obeys Byerlee's Law. Further, velocity-step experiments indicate that the frictional coefficient at steady-state increases when the rate of displacement increases (velocity-strengthening). It was, therefore, suggested that stable sliding is preferred in the shallow portion of the Hayward Fault. Indeed, that portion of the fault has been observed to creep (stable sliding) from geodetic measurements. We would like to emphasize that it is also important to investigate the physical properties of fault rocks in outcrop, in order to obtain a preliminary understanding of fault systems, such as the studies by *Morrow and Lockner* [2001], provided that the rocks are neither significantly weathered nor include many secondary minerals.

The Nankai Trough region is considered to be a candidate site for drilling into a seismogenic zone. As a preliminary study for the drilling program, we have conducted a series of permeability measurements and shear failure experiments in seismogenic environments using basalt sampled at the outcrop of an exhumed fault zone in the Cretaceous Shimanto accretionary complex, in Shikoku, SW Japan. This area provides a unique opportunity to study the mechanical and fluid transport properties of an ancient subduction zone fault [*e.g.,* Onishi *et al.,* 2001, Sakaguchi *et al.,* 2002]. Investigating the transporting properties of subduction zone faults is important for understanding shear strength and slip-stability, or instability, of subduction zone faults. The results show that basalt in the fault zone rapidly becomes sealed after a shear failure, due to the precipitation of clay-like minerals, and indicate the potential for a high fluid pressure during the majority of interseismic periods.

Experimental Method

Alternating basalt in the Cretaceous Shimanto accretionary complex in Shikoku, SW Japan, was chosen as the specimen for this study. It includes mineral vein networks composed of ankerite, quartz, chlorite, calcite, etc. This basalt is located in the shear zone between the sandstone-dominant coherent unit of the Nonokawa Formation and the Okitsu Melange. Thermal conditions around this area, which have been measured by vitrinite reflectance, reveal that the maximum temperature in the past ranged up to 230℃±30℃, on average [Sakaguchi, 1999]. This indicates that the basalt would have been in the seismogenic zone during underthrusting or accretion. Ikesawa *et al.,* [2003] discovered pseudo-tachylyte in the shear zone between the coherent unit of the Nonokawa Formation and the Okitsu Melange, close to where our specimens were collected. It is suggested that the vein minerals, such as quartz and ankerite, around the fault zone have a close relationship with dynamic fault slip [Sakaguchi *et al.,* 2002]. We, therefore, consider that the vein minerals in the sampled basalt were formed in the seismogenic zone, not at the surface.

The average porosity and density of the basalt are estimated to be 0.1%, and 2.73 g/cm³, respectively. Cylindrical test specimens (length=40 mm, diameter =20 mm) were cored in the same direction from the sampled block, to an accuracy of within 0.02 mm. To saturate the specimens with water before the experiments, they were submerged in distilled water after having been kept in a container that was evacuated with a vacuum pump for 6〜8 hours. Water saturation of the interstitial pores occurred after about 5 days.

All experiments were conducted in a triaxial pressure apparatus at the Earthquake Research Institutive, University of Tokyo. Details of the apparatus are given in Ohnaka *et al.,* [1997] and Kato *et al.,* [2003]. The confining pressure P_c, pore water pressure P_p and temperature $T,$ range up to 500 MPa, 400 MPa and 500℃, respectively. The effective confining pressure is, however, limited to 150 MPa for permeability measurements, because of the low yield strength of the tube that is used as a fluid conduit inside the pressure-vessel. A cylindrical rock specimen was jacketed by a silver sleeve, and loaded in the apparatus. To ensure that there was no flow between the silver sleeve and the surface of the specimen, we conducted a test with a dummy speci-

men of stainless steel. We applied a pore pressure difference (3 MPa) between the top and bottom faces of the stainless steel specimen, and found no pressure leak occurring during the period of half a day. The flow of water through the specimen was driven by a fluid intensifier. A transient pulse test was applied to measure permeability. Our apparatus has two reservoirs with volumes of 60 cm^3 and 90 cm^3, which enable us to conduct the transient pulse test proposed by Brace *et al.* [1968]. The difference of pore pressure between inlet and outlet needs to be small to evaluate permeability correctly. A pore pressure differential of around 2 MPa was imposed between the inlet and the outlet of the specimen as a pulse. The lower limit of accuracy for our measuring system is around 0.8×10^{-21} m^2.

We investigated the dependence of permeability on the effective confining pressure at room temperature and 250℃. Subsequently, the specimen was loaded at a strain rate of $(0.2 \sim 1.0) \times 10^{-5}$/s [Table 1], resulting in its fracturing at $P_c = 140$ MPa, $P_p = 105$ MPa, and $T = 250$℃, simulating a depth of around 6 km from the surface of the accretionary prism [Sakaguchi, 1999]. We then measured the permeability evolution following the shear failure over the course of approximately 2 days. The failure specimens were kept with no shear stress under hydrothermal conditions. During the permeability evolution experiment, permeability was evaluated by reversing the 2 MPa fluid pressure gradient. In this way, the same volume of fluid flowed back and forth through the specimen [Moore *et al.,* 1994].

Experimental Results

Figure 1 shows an example of the permeability measurements for various pore water pressures using intact basalt at room temperature. The confining pressures are the same ($P_c = 140$ MPa) for the four tests, with different average pore pressures. It was found that the time decay constant increases with an increase in effective confining pressure P_c^{eff}. The pressure difference ΔP between the inlet P_{p2} and outlet P_{p1} is expressed as a function of time by

$$\Delta P(t) = P_{p2}(t) - P_{p1}(t) = \Delta P_o \exp(-t/\tau),$$

where

$$1/\tau = kS(1/V_{r1} + 1/V_{r2})/(\mu\beta L),$$

S is cross-sectional area, L is length of the specimen, V_{r2} and V_{r1} is the volume of each reservoir at inlet

and outlet, μ is the viscosity of fluid, and β is defined as the total compressibility including fluid and measurement system. The value of β was determined by measuring the decrease in the volume of fluid against the pressure step before each permeability measurement. The decay time constant τ was evaluated by the least squares method, and permeability was obtained using the above equation (broken lines in Fig. 1).

Figure 2 (a) plots the permeability measured at room temperature versus effective confining pressure P_c^{eff}, for five specimens. The measurements for each specimen were conducted in the order indicated by the arrow in Fig. 2 : loading first and unloading afterward. Values from loading were higher than during unloading due to time-dependent relaxation processes, as is characteristic of many rocks and granular materials. Note that the permeability measurements display a drop as P_c^{eff} increases [*e.g.,* Wibberley and Shimamoto, 2003]. The relation between permeability, $k,$ and P_c^{eff} is approximated by an exponential corresponding to a linear line in Fig. 2 (a). The pressure-sensitivity of permeability, which is defined as $-\Delta \log_{10}k/\Delta P_c^{\text{eff}}$, ranges from 0.01 to 0.028, within the measured effective confining pressures. The permeability at room temperature roughly ranges from 10^{-17} to 10^{-21} m^2 at $P_c^{\text{eff}} = 100$ MPa. Because the sampled block was weathered, the structures of crack-network or porosity vary from place to place in the sampled block.
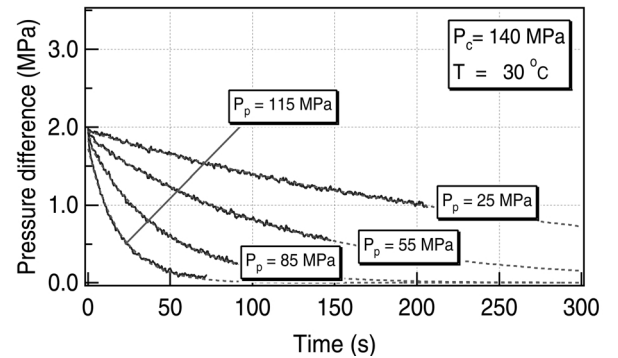
Afterward, each specimen was heated to 250℃.

Fig. 1. A plot of typical examples of the measured data for the transient pulse test at confining pressure $P_c = 140$ MPa and room temperature. Changes in the pore pressure difference between the inlet and the outlet are shown for various pore water pressures. The broken line denotes the least squares fit curve to the data.

The permeability measurements at 250℃ are plotted against P_c^{eff} in Fig. 2 (b), where the sample number corresponds to the same sample shown in Fig. 2 (a). The broken line in the figures denotes the measurement limit of our system. It was found that permeability at 250℃ decreases on the whole, compared to that at room temperature. Although the thermal cracking caused by an increase in temperature produces conduits for pore water transfer, the decrease in permeability tested in this study indicates that precipitation sealing is induced by changing temperature conditions or by primary mineral dissolution. Note that the permeability after unloading converges to a value less than $10^{-20} \sim 10^{-21}$ m².

Shear failure experiments were conducted under the conditions $(P_c, P_p, T) = (140\,\text{MPa}, 105\,\text{MPa}, 250℃$ or room temperature), after measuring permeability. The peak value of the differential axial stress for each sample roughly ranges from 280 MPa to 450 MPa [Table 1]. When the shear failure experiment was completed, the shear load was unloaded, and the specimen was kept under the conditions $(P_c, P_p, T) = (140\,\text{MPa}, 105\,\text{MPa}, 250℃$ or room temperature) for permeability evolution measurement (Sample 1, 2, and 4). The permeability evolution data after the shear failure is shown in Fig. 3. In the results for 250℃, note that significant reductions in permeability are observed in a short period. The permeability reduction at 250℃ is approximately 2~3 orders over about 50 hours, and the specimens were progressively sealed during the hold period. Conversely, permeability at room temperature is virtually constant against hold time, or shows only a slight decrease. Therefore, the permeability reduction at higher temperatures is more significant than that at lower temperatures.

When the samples showing a permeability reduction with hold time (Sample 1 in Fig. 3) were removed from the silver jacket at the end of the experiment, the two sides of the failure specimen had to be forcefully separated by hand, which indicates that a small amount of healing around failure surfaces occurred during the hold period.

Microscopic Observations

Unpolished broken chunks of the fault zone from the specimen tested at 250℃ were examined by scanning electron microscopy (SEM) to characterize the grain surfaces. Fig. 4 (a) shows evidence of the precipitation of secondary minerals. Platy minerals appear as a widespread mesh-like coating, although
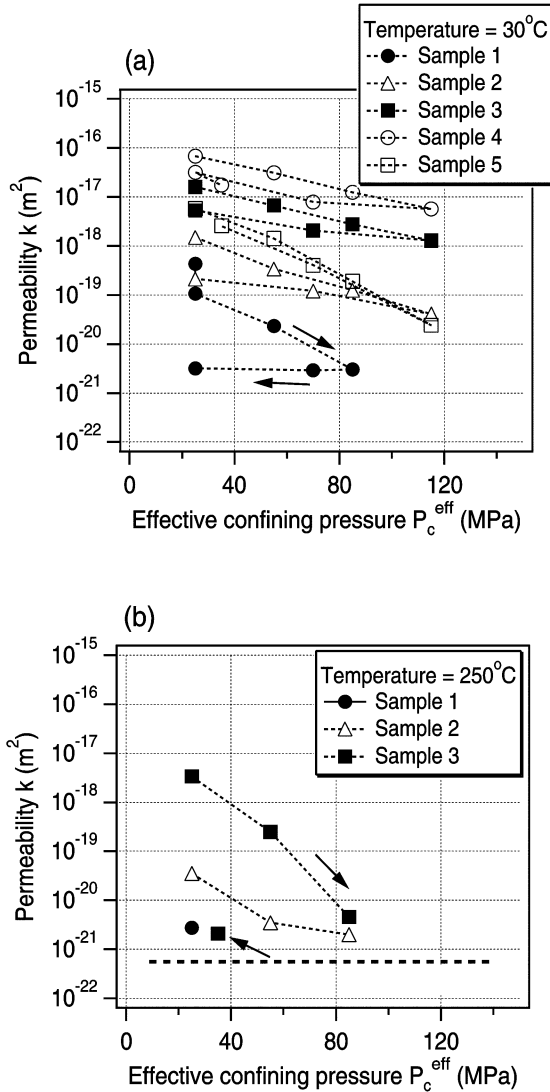

Fig. 2. Permeability, *k,* as a function of effective confining pressure : (a) at room temperature, (b) at 250℃. The broken line in (b) indicates the measurement limit of permeability for our system.

Table 1. Peak differential axial stress of each sample at selected strain rates and temperatures.

	Temperature (℃)	Strain rate (1/s)	Peak Axial stress (MPa)
Sample 1	250	10^{-5}/s	443
Sample 2	250	10^{-5}/s	341
Sample 3	250	10^{-5}/s	284
Sample 4	30	0.25×10^{-5}/s	282
Sample 5	30	10^{-5}/s	353

they did not form everywhere. Because of the extremely fine-grained nature and the fragility of these minerals, a microprobe analysis could not be used to determine their elemental composition. Energy-dispersive X ray measurements (EDS) using SEM, however, indicate that they are mainly composed of Si, Al, Na, and Ca. The habit of the visible secondary minerals is similar in appearance to minerals identified as belonging to the chlorite or smectite group by other researchers [e.g.,1 Hajash and Bloom, 1991, Tenthorey et al, 1998]. For the broken chunks collected from the sample tested at room temperature (sample 4), the platy minerals that had been observed as mesh-like coating at 250℃ were not frequently observed (Fig. 4 (b)). Another method is necessary to demonstrate the chemical formula of the precipitated minerals.

Discussion

One may argue that the permeability of one sample tested at room temperature (Sample 4) decreased slightly after shear failure (Fig. 2, 3), which differs from the results for other samples (Sample 1, 2) that showed an increase in permeability after failure. In Sample 4, comminution of the fault gouge during displacement appears to have caused a reduction in permeability after failure. However, note that the permeability of Sample 4 was initially high ($\sim$

$10^{-17}\,\mathrm{m^2}$). By contrast, the permeability of Samples 1 and 2 was initially low ($\sim 10^{-21}\,\mathrm{m^2}$) before the shear load was applied. Even though the fault surfaces of Samples 1 and 2 were filled with comminuted gouges after shear failure, the total permeability of the samples increased compared to that before failure. Whether the permeability of a sample increases or not following shear failure depends on both the initial value of permeability and the hydraulic properties of the comminuted gouge filled failure surfaces.

Following shear failure, a reduction in the permeability of basalt with time was found at elevated temperatures. However, only a slight healing of the failure surfaces was observed. Microscopic observations indicate that the permeability reduction was
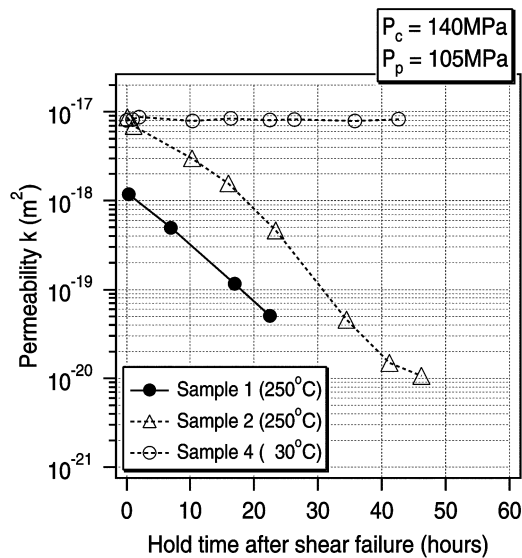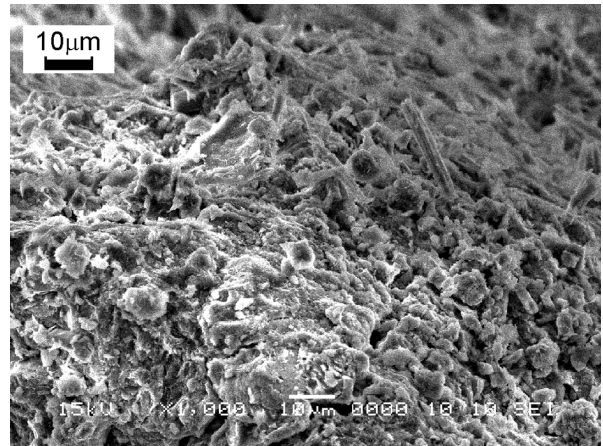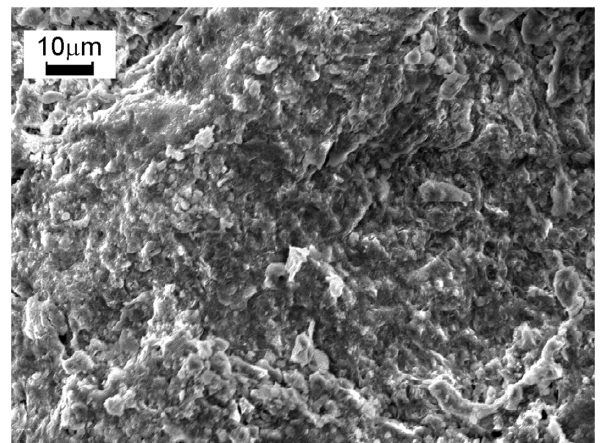

(a)

(b)

Fi. 4. Scanning electron micrographs showing a fragment of failure gouge material after the permeability evolution test. (a) Sample 2 at 250℃. (b) Sample 4 at 30℃.

Fig. 3. Permeability evolution data from the experiments conducted after shear failure at $P_c=$ 140 MPa and $P_p=105$ MPa. Open circles denote data at room temperature, and other symbols indicate measurements at 250℃.

induced by precipitation sealing by clay-like minerals. It is suggested that sealing is a result of secondary mineral precipitation and that healing results from the cementation of grains by the precipitating minerals [*Olsen and Scholz*, 1998] Thus, the results of sealing and healing in this paper indicate that while the precipitating minerals cause rapid sealing, the cemented minerals are not very strong. We consider that the cementation of more cohesive minerals such as quartz, requires significantly longer time-scales to be completed, and that the cementation of such minerals will cause sufficient healing of the fault surface for the next earthquake. It is, therefore, necessary to conduct permeability evolution experiments following shear failure for longer periods than in the present study.

Time-variations in pore fluid pressure and permeability of the fault zone are very important elements of fault behavior. *Sleep and Blanpied* [1992] modeled variations of pore fluid pressure during the interseismic period. It was suggested that pore fluid pressure gradually rises, resulting in a reduction of the shear strength of the fault. Immediately following rupture, pore fluid pressure rapidly decreases and the cycle begins again. The rise in pore fluid pressure during an interseismic period is due to the compact creep of the fault zone. However, the reduction of permeability is considered to be due not only to the compact creep mechanism, but also to precipitation of clay-like minerals [*Olsen and Scholz*, 1998]. It is inferred from this study that the permeability of a subduction megathrust fault would rapidly decrease after shear rupture at elevated temperatures, because of fault sealing. Then, the pore fluid pressure would be kept high, or close to lithostatic pressure, during the majority of the interseismic period. This leads to the expectation that the shear strength of a subduction megathrust fault is weak. Many previous studies have suggested that subduction zone megathrusts are weak faults. Potential causes of this apparent weakness include : (a) intrinsically weak materials present in the fault zone, (b) elevated fluid pressure resulting in low effective normal stress conditions, and/or (c) dynamic weakness generated during rapid slip events [*Nankai Trough Seismogenic Zone Research Group*, 2001]. Our study suggests that the elevated fluid pressure caused by fault sealing results in low effective normal stress conditions dur-

ing interseismic periods. To complete the picture of permeability structure and pore fluid pressure evolution during the interseismic period of a mega-thrust earthquake, permeability measurements using coherent-unit sandstone and mudstone from the Melange need to be conducted in the future. Care should be taken as permeability values estimated in the laboratory show the minimum value at field scales, because permeability is dependent on scale. Thus, the relative values of permeability measured in the laboratory will give us meaningful information on the permeability structure around megathrust fault zones.

Conclusions

The permeability of basalt from an ancient subduction-zone fault decreases with increasing effective confining pressure and temperature, although the absolute value depends on the extent of cracking induced by weathering in the specimen. Rapid sealing at elevated temperatures was observed during the hold experiments following shear failures of the samples. However, only slight healing of the shear zone occurred. SEM observations provide evidence for the precipitation of clay-like minerals. These results indicate that the permeability of a subduction megathrust fault would rapidly decrease due to the precipitation of clay-like minerals and other minerals, and shows the potential for high fluid pressure in the fault zone.

Acknowledgments

Reference
Blanpied, M.L., C.J. Marone, D.A. Lockner, J.D. Byerlee and D.P. King, Quantitative measure of the variation in fault rheology due to fluid-rock interactions, *J. Geophys. Res.,* **103**, 9691–9712, 1998.
Brace, W.F., J.B. Walsh and W.T. Frangos, 1968, Permeability of granite under high pressure, *J. Geophys. Res.,* **73**, 2225–2236.
Hajash, A. and M.A. Bloom, 1991, Marine diagenesis of feldspathic sand : A flow-through experimental study at 200℃, 1 kbar, *Chem. Geol.,5* **89**, 359–377.
Ikesawa E., A. Sakaguchi, G. Kimura, 2003, Pseudotachylyte

from ancient accretionary complex : Evidence for melt generation during seismic slip along a master decollement?, in press, *Geology.*

Kato, A., M. Ohnaka and H. Mochizuki, 2003, Constitutive properties for the shear failure of intact granite in seismogenic environments, *J. Geophys. Res.,* 108B1, 2060, doi : 10.1029/2001JB000791.

Moore D.A., D.A. Lockner and J.D. Byerlee, 1994, Reduction of permeability in granite at elevated-temperatures, *Science,* **265**, 1558–1561.

Morrow C.A. and D.A. Lockner, 2001, Hayward fault rocks : porosity, density and strength measurements, *USGS Open-File Report,* 01–421.

Nankai Trough Seismogenic Zone Research Group, 2001, *Preliminary IODP Proposal.*

Onishi, C.T., G. Kimura, Y. Hashimoto, K. Ikehara-Ohmori and T. Watanabe, 2001, Deformation history of tectonic melange and its relationship to the underplating process and relative plate motion ; an example from the deeply buried Shimanto Belt, SW Japan, *Tectonics,* **20**, 376–393.

Ohnaka, M., M. Akatsu, H. Mochizuki, A. Odera, F. Tagashira and Y. Yamamoto, 1997, A constitutive law for the shear failure of rock under lithospheric conditions, *Tectonophysics,* **277**, 1–27.

Olsen, P.M. and C.H. Scholz, 1998, Healing and sealing of a simulated fault gouge under hydrothermal conditions : Implications for fault healing, *J. Geophys. Res.,* **103**, 7421–7430.

Sakaguchi, A., 1999, Thermal structure and paleo-heat flow in the Shimanto accretionary prism, Southwest Japan : *Island Arc,* **8**, 359–372.

Sakaguchi, A., R. Takami, E. Ikesawa and T. Kanaya, 2002, Tectonic setting of seismogenic fault in the ancient subduction zone, Okitsu Melange, Shimanto accretionary complex, SW Japan, submitted to *Tectonics.*

Sleep, N.H. and M.L. Blanpied., 1992, Creep, compaction and the weak rheology of major faults, *Nature,* **359**, 687–692.

Tenthorey, E., C.H. Scholz and E. Aharonov, 1998, Precipitation sealing and diagenesis, *J. Geophys. Res.,* **103**, 23951–23967.

Wibberley, A.J.C. and T. Shimamoto, 2003, Internal structure and permeability of major strike-slip fault zone : the Median Tectonic Line in Mie Prefecture, Southwest Japan, *J. Struct. Geol.,* **25**, 59–78.